Construction and Building Materials 264 (2020) 120241

Contents lists available at ScienceDirect

Construction and Building Materials

journal homepage: www.elsevier.com/locate/conbuildmat

Evaluating the effects of nanosilica on the material properties of lightweight and ultra-lightweight concrete using image-based approaches

Pawel Sikora [a,b], Teresa Rucinska [b], Dietmar Stephan [a], Sang-Yeop Chung [c,*], Mohamed Abd Elrahman [a,d,*]

[a] Building Materials and Construction Chemistry, Technische Universität Berlin, Germany
[b] Faculty of Civil Engineering and Architecture, West Pomeranian University of Technology Szczecin, Szczecin, Poland
[c] Department of Civil and Environmental Engineering, Sejong University, South Korea
[d] Structural Engineering Department, Mansoura University, Mansoura, Egypt

HIGHLIGHTS

- Lightweight aggregate concretes (LWACs) with a targeted density of 850 kg/m^{3,} and 450 kg/m^3 were developed.
- Cement was replaced with 1, 2, 5 and 10% nanosilica (by mass of cement).
- Shrinkage, transport, mechanical and microstructural (2D and 3D) properties of concretes were evaluated.
- Nanosilica has a beneficial effect in improving the mechanical and transport properties of concretes.
- Nanosilica significantly improves the pore characteristics of lightweight concretes.

ARTICLE INFO

Article history:
Received 27 April 2020
Received in revised form 28 June 2020
Accepted 8 July 2020
Available online 30 July 2020

Keywords:
Light-weight concrete
Ultra-lightweight concrete
Mechanical performance
Drying shrinkage
Porosity
Nanosilica
micro-CT
RapidAir
Thermal conductivity
Thermal insulation

ABSTRACT

This work is aimed at characterizing the effects of nanosilica (NS) on the properties of lightweight aggregate concretes with different densities. Lightweight aggregate concrete (LWAC) and ultra-lightweight aggregate concrete (ULWAC) with targeted oven-dry densities of 850 kg/m^3 and 450 kg/m^3, respectively, were produced. The mixtures were modified by replacing cement with nanosilica, in concentrations of 1, 2, 5 and 10 wt-%. For comparison purposes, control specimens containing either cement alone or cement with silica fume (SF) were also produced. Their mechanical properties, including flexural and compressive strengths and transport characteristics, were evaluated by measuring the water accessible porosity and water absorption coefficients of the concretes. In addition, the thermal conductivity and drying shrinkage, being important parameters of lightweight concrete, were characterized. The pore structure characteristics of the concretes were assessed using 2D and 3D image analysis techniques; namely, using an automated air void analyser and micro-computed tomography (micro-CT), respectively. The experimental results show that NS has a significant effect on improving the mechanical and transport properties of lightweight concretes and that the efficiency of NS is much higher than that of SF. Moreover, depending on dosage, NS was found to have a negligible or decreasing influence on the drying shrinkage of concrete, after 28 days of curing. Microstructural studies confirmed that NS significantly affects the pore characteristics of concretes, thus resulting in concretes with denser and stronger microstructures.

1. Introduction

Lightweight concrete (LWC) is a widely used structural and masonry element in the construction field. It attributes its popularity to low density, as well as to substantial acoustic and thermal insulation properties. The use of LWC decreases the total weight of a structure, where the mass of concrete is often considered to be responsible for more than half of the dead load of a construction. According to EN 206-1 [1], the oven-dry density of

* Corresponding authors at: Building Materials and Construction Chemistry, Technische Universität Berlin, Gustav-Meyer-Allee 25, 13355, Berlin, Germany (M. Abd Elrahman); Department of Civil and Environmental Engineering, Sejong University, Seoul 05006, Republic of Korea (S.-Y. Chung).
E-mail addresses: sychung@sejong.ac.kr (S.-Y. Chung), mohamedattia@mans.edu.eg (M. Abd Elrahman).

https://doi.org/10.1016/j.conbuildmat.2020.120241
0950-0618/

lightweight concrete should be in the range of 800–2000 kg/m^3. However, developments in recent decades have already made it possible to produce concretes with a density lower than 800 kg/m^3 with this material often referred to as ultra-lightweight concrete (ULWC). Despite the beneficial properties of LWCs mentioned above, this material has certain disadvantages, such as low mechanical strength and high water absorption, which are effects of noticeably increased porosity, induced by the porous nature of the aggregates used and by air entrainment. Moreover, LWC starts to shrink when dried, leading to cracks from tensile stresses which are generated [2,3], as the concrete volume decreases significantly due to water in the small capillary pores being lost. The presence of aggregates hinders this contraction and restrains paste shrinkage, thus making the concrete more stable. Accordingly, the use of weak and less rigid aggregates with low elastic moduli reduces the effect, leading to a significant increase in the volume of shrinkage, as in the case of LWCs [4,5]. Moreover, the high amount of cement paste used in LWCs, either for the purposes of workability or strength, increases shrinkage.

However, the water absorbed by lightweight aggregates (LWAs) reduces concrete shrinkage [6], with the LWAs thus acting as reservoirs which compensate for the loss in moisture due to drying. Such so-called internal curing can reduce lightweight aggregate concrete (LWAC) shrinkage significantly [5]. In addition, the strong bond between LWA and the cement matrix reduces length changes caused by moisture movements or thermal effects [7]. A combination of these parameters, as well as the wide variety of LWAs, make the shrinkage behavior of LWAC different from that of normal-weight concrete [2,7]. Also, mix composition has a strong influence on shrinkage cracking and the use of different types of aggregates results in very different concrete shrinkage behavior. It has been reported that, as the modulus of elasticity of an aggregate decreases, shrinkage values increase.

In most lightweight concrete mixes a high content of cementitious materials is used to achieve the required mechanical properties; consequently a high hydration heat and subsequent high shrinkage occur [5]. Several supplementary cementitious materials (SCMs), particularly ground granulated blast-furnace slag (GGBFS), fly ash (FA) or silica fume (SF), can be included to reduce these harmful effects and to achieve the required strength, with minimum negative influence on other properties. SF has proved to be the most effective SCM for improving the performance of LWACs but it has a negative effect on drying shrinkage [4].

Although the effects of the commonly used SCMs have been relatively well established regarding LWC performance, significant developments in the field of concrete technology have recently lead to the production of a whole variety of new admixtures and additives [8–10].

Nanomaterials have garnered substantial interest from research and industry around the world in the last two decades. As nano-sized admixtures possess spectacular surface reactivity, attributed to their ultra-fine size and high specific surface area, they exhibit substantially higher reactivity than conventional SCMs and thus increase the performance of cement-based composites which utilize them, at lower amounts [10]. Among the nanomaterials used for the formulation of building materials, nanosilica (NS) has gained substantial interest, with a few commercial products already available on the market. The effects of NS on concrete are comparable to that of silica fume, but due to its ultrafine size and high chemical reactivity, its performance is much better with a lower amount of admixture required [11,12]. In general, the improvement can be attributed to the acceleration of cement hydration (seeding-effect), the fast pozzolanic reaction, as well as to the optimized packing of the particles in the cement matrix [13–15]. Beside, beneficial effect of NS on the the early age properties of cementitious composites [16–19], it also makes a substantial contribution to time dependant properties as a result of its high pozzolanic activity [20–23]. Various authors have shown that NS has a much higher reactivity than conventional SF, with a lower dosage necessary to achieve comparable or better concrete properties [11,12,24–25]. While knowledge regarding the effects of NS on the properties of normal-weight cementitious composites is widely established, only a few works are available on this topic, indicating that NS can be useful in the production of LWCs with advanced mechanical and durability-related properties.

As far as the authors of this paper are aware, only limited work has been done in this field, with nanosilica dosages ranging from a very low 0.1 wt-%, up to a very high 10 wt-%. The available studies related to the production of LWAC containing NS are summarized in Table 1.

In a study by Zhang et al. [26], a low dosage of NS (from 0.1 to 1 wt-%) was incorporated into LWAC. A significant improvement in both early (7 d) and standard (28 d) flexural and compressive strength improvement was reported, with a small dosage of NS (0.1–0.2 wt-%). The authors reported that exceeding the optimal dosage lead to a neutralization of the effects of NS, with specimens exhibiting strengths comparable to that of the control specimen. A slightly higher dosage of NS was evaluated in the work of Du et al. [27]. They evaluated structural LWACs which were incorporated with 1 or 2 wt-% of NS. The authors reported early flexural and compressive strength improvements (after 1 d and 7 d) with curing, when NS was present in the mixture, although 28 d strength improvements were not reported. A decrement in water accessible porosity, water penetration depth, water sorptivity, as well as higher resistance against chloride ion penetration, were also reported for NS-modified specimens. In another work [13], the effects of 1, 2 and 3 wt-% of NS on the compressive strength development, shrinkage and cracking sensitivity of LWACs were evaluated. Compressive strength improvement was found to have occurred at every testing date, with the largest effect observed in early strength improvement. Moreover, no significant influence on the long-term shrinkage of LWAC was found, while evaluations of early cracking sensitivity showed that, with increasing NS dosage, the total LWAC cracking area decreased continuously. Bogas et al. [6] studied the influence of fine materials on the shrinkage of LWC and compared the results to normal-weight concrete (NWC). They found that the shrinkage of LWC is much higher than that of NWC. In addition, LWC shrinkage is proportioned negatively to aggregate volume. Their experimental results revealed that the long term shrinkage of nanosilica is lower than that of silica fume. A comparative study undertaken by Atmaca et al. [28] showed that 3 wt-% of NS in LWAC is beneficial in improving compressive strength, split tensile strength, water sorptivity and gas permeability of high-strength LWAC. The effect of NS was more pronounced in normal concrete than in concrete containing LWA. An interesting evaluation regarding the fresh and hardened properties of self-compacting structural LWAC, containing 1, 3, and 5 wt-.% of nanosilica, has been presented in the work of Afzali Naniz and Mazloom [29]. For comparison, they also produced a reference specimen with 10 wt-% of SF. By undertaking an extensive evaluation of the fresh properties of concrete, they showed that the replacement of cement with either NS or SF decreased the fluidity of self-compacting lightweight concrete, thus necessitating a high dosage of superplasticizer (SP). Moreover, they reported that the presence of either SF or NS reduced bleeding in concrete. A higher NS dosage improved the mechanical performance of the concretes. However, the best performance was obtained when a ternary mixture, containing both SF and NS, was produced. Similar conclusions, regarding the fresh properties of much lighter (density < 1000 kg/m^3) self-compacting LWAC, were recently reported by Abd Elrahman et al. [30]. Their study on the effects of 1, 2, and 4 wt-% of NS on LWAC containing expanded glass aggregate showed that an increment in NS dosage leads to a

Table 1
Summary of available studies related to the incorporation of nanosilica in LWCs.

Ref.	Dosage of nanosilica [wt.-%]	Oven-dry density [kg/m^3]	Tested properties	Optimal dosage [wt-%]	Effects	Type of LWA and w/c or w/b ratio
[26]	0, 0.05, 0.1, 0.2, 0.5, 1.0	~1000*	Flexural strength (7, 28 d), compressive strength (7, 28 d)	0.1–0.2	Improved early and 28 days flexural and compressive strength	Expanded shale ceramsite w/c = 0.45
[27]	1, 2	1845–1900	Compressive strength (1, 7 and 28 d), water accessible porosity, water sorptivity, water penetration depth, rapid chloride penetration test, chloride diffusion test, rapid chloride migration test	1	Early compressive strength improvement (1 d and 7 d), 28 d strength not affected. Decreased water accessible porosity, water penetration depth, water sorptivity and higher resistance against chloride ion penetration	Expanded clay spheres coarse aggregate w/c = 0.42
[13]	1, 2, 3	1800–1900*	Compressive strength (3, 7, 28 d), long-term shrinkage, early cracking sensitivity	3	Early and final strength improvement, no significant influence on the long-term shrinkage, total cracking area decreased	Fly-ash clay ceramsite or shale ceramiste w/b = 0.35
[29]	1, 3, 5	1800–1900*	Compressive strength (28 d), split tensile strength (28 d) and flexural strength (28 d), Ultrasonic pulse velocity, electrical resistivity	3–5	Strength improvements, improvement of ultrasonic pulse velocity and electrical resistivity	Expanded clay aggregate w/b = 0.35 and w/b = 0.45
[30]	1, 2, 4	915–955	Flexural strength (7, 28, 90 d) and compressive strength (7, 28, 90 d), water accessible porosity, water sorptivity, microstructural properties, thermal conductivity	4	Improved of early and long term flexural and compressive strength, decreased water accessible porosity and water sorptivity, improved microstructure and decreased total porosity of cement paste	Expanded glass aggregate w/b = 0.40
[31]	1,2,3	1075–1240	Compressive strength (1, 2,7, 28 and 91 d), water sorptivity, rapid chloride permeability test, water penetration, chloride diffusion test, water accessible porosity	2	Improved early and long term compressive strength, improved water absorptivity, water accessible porosity and chloride diffusion,	Containing cenospheres and expanded glass aggregates (up to 2 mm). w/b = 0.32 and w/b = 0.24
[28]	3	2000–2100*	Compressive strength (3, 7, 28 and 90 days), split-tensile strength (28 and 90 days). water sorptivity and gas permeability	3	Compressive strength and split-tensile strength improved in all ages tested. Decrement in water sorptivity and gas permeability	Cold-bonded aggregate (90% fly ash + 10% cement) w/b = 0.35
[32]	5, 10	650–700	Compressive strength (7, 28 d), thermal conductivity	10	Improvement of 7 and 28 d compressive strength, no effect on thermal conductivity	Expanded recycled glass lightweight
[33]	10	900–1000*	Compressive strength (7, 28 d), water absorption, sulfate resistance	10	Improvement of 7 and 28 d compressive strength, decreased water absorption, decreased expansion due to sulfate attack	Perlite, thermally expanded clay aliven, w/b = 0.35

*Estimated values. Exact oven-dry density values were not provided in the manuscript and density range was therefore calculated indirectly, based on the available mixture formulas or measurements.

significantly increased demand for superplasticizer. However, the mixture produced in this case was more cohesive, thus necessitating a lower amount of stabilizer. In the case of hardened properties, specimens containing > 1 wt-% of NS exhibited flexural and compressive strength improvements from the early days of curing. In the work of Du [31], the author evaluated the effects of 1, 2 and 3 wt-% of NS on the properties of LWAC in the density range of 1075–1240 kg/m^3, showing that when the optimal amount of NS is incorporated (2 wt-%), a substantial improvement in strength development from, the first day hydration, can be observed, as well as lower water adsorption and chloride penetration. Higher dosages of NS on the properties of LWAC have been evaluated in the work of Yu et al. [32]. Namely, they examined the effects of 5 and 10 wt-% of NS on the properties of ultra-lightweight aggregate concretes (ULWACs) containing different amounts of cement (350, 400, and 450 kg/m^3) and expanded recycled glass lightweight aggregate. They found that specimens incorporated with 10 wt-% of NS exhibited approximately 20% higher compressive strength values than the control. Vargas et al.'s [33] work on the effects of replacing cement with 10 wt-% of NS, on the compressive strength of two types of LWACs, showed that the NS-incorporated specimens exhibited similar 28-day strengths to that of plain cement. They concluded that the mechanical performance of LWAC is dependent only on the type of aggregate used. Moreover, due to refinement of the cement paste microstructure by nanosilica, the NS-incorporated samples exhibited a lower volume of voids and a decreased water absorption rate.

The literature review above shows that research in the field has focused on the evaluation of mechanical performance, along with certain durability related issues. In contrast, less attention has been paid to drying shrinkage or the microstructural characterization of lightweight concretes, with certain factors, such as NS content (low dosage vs. high dosage), yet to be comprehensively evaluated. In addition, knowledge in this field is mainly limited to the potential structural applications of higher density LWCs. In contrast, this study aims at shedding light on the design and performance of lightweight and ultralightweight aggregate concretes modified with nanosilica, which might find further utilization in non-structural applications, such as insulating concrete.

The study examines the influence of nanosilica addition, with varied content ranging from 1 wt-% to 10 wt-% of cement replacement, on the properties of lightweight aggregate concretes (LWACs) with two target densities of 450 kg/m^3 and 850 kg/m^3. For comparison purposes, a specimen with SF was produced as a control mix. The paper also evaluates mechanical performance, transport properties and drying shrinkage. Microstructural evaluations, including 2D and 3D imagining techniques, are also applied so as to characterize the effects of NS on the pore structures of the ULWCs produced.

2. Materials and methods

2.1. Raw materials

Lightweight concrete is characterized by its low thermal conductivity. As such, cement with slow hydration should be used in a mix design, to reduce thermal micro-cracking due to the evolution of heat from cement hydration. Slag cement CEM III/A 42.5 N, in accordance with EN 197-1 [34] and provided by HeidelbergCement AG (Heidelberg, Germany), was therefore used. Expanded glass (Liaver) with different fractions (0.5–1, 1–2, and 2–4 mm) was used as a lightweight aggregate (Liaver GmbH & Co.KG, Ilmenau, Germany), due to its high strength/density ratio compared to other types [35]. Condensed silica fume, in accordance with EN 13263-1 [36] (Sika GmbH, Stuttgart, Germany), was also used to improve concrete the strength development and to compare its performance with nanosilica. Fine quartz sand (0.1–0.3 mm) was used in the lightweight concrete mixes to achieve the targeted density (Sand-Schulz GmbH, Berlin, Germany) , without using a high amount of active powder. Tables 2 and 3, respectively, show the physical properties of the fine materials and lightweight aggregates used.

A commercially available colloidal silica suspension, Levasil CB8 (Nouryon, Sweden), was used in this study. The liquid phase in the NS suspension was also considered to be a part of the mixing water used to prepare concrete (see Section 2.2). Details of the NS used in this study are presented in Table 4 and have been described comprehensively elsewhere [37].

2.2. Mixture design

Two series of lightweight aggregate concretes, with two targeted density classes of 450 kg/m^3 and 850 kg/m^3, were investigated in this study. The concrete mixture proportioning was based on the packing density concept, with aggregate grading being an important parameter that can affect the properties of concrete in both fresh and hardened states [35]. Optimization of the ingredient grading improves the packing of the whole skeleton, enhances workability, reduces the amount of cement paste required to fill the voids between aggregate particles and consequently improves compressive strength. Several models and formulas have been developed to optimize the granulation of solid materials [38]. To calculate mixture composition in this investigation, the model developed by Andresean and Andersen was applied (Eq. (1)):

$$P(D) = \frac{D^q - D_{min}^q}{D_{max}^q - D_{min}^q} \quad (1)$$

where P(D) is the total fraction passing through a sieve with an opening size D, D_{max} is the maximum particle size, D_{min} is the minimum particle size and q is the distribution factor [39,40].

The distribution factor is an important parameter in regard to grading characteristics, with a small q representing a high amount of fines and a high q pointing to a coarser mixture with a low fines

Table 2
Properties of the fine materials used.

Material	CEM III/A 42.5 N	Silica fume	Quartz sand
Specific density [g/cm^3]	3.03	2.20	2.67
Surface area (Blaine) [cm^2/g]	4180	200,000	780

Table 3
Properties of the lightweight aggregates used.

Material	Liaver® 0.5–1 mm	Liaver® 1–2 mm	Liaver® 2–4 mm
Bulk density [kg/m^3]	250	220	190
Particle density [kg/m^3]	450	350	320
Crushing resistance [N/mm^2]	>2.6	>2.4	>2.1
Water absorption [wt. %]	15.4	15.8	14.4

Table 4
Colloidal silica properties.

Particle size*	Solid content	Density	Viscosity	pH
10–140 nm	50 wt-%	1.4 g/cm^3	8 cP	9.5

*Based on TEM analysis.

content. A small q is not ideal in achieving ultra-lightweight concrete with a density of 450 kg/m^3, because of the high density of fine lightweight aggregates (0.5–1 mm), as compared to the density of coarser lightweight aggregates (2–4), as can be seen in Table 2. What is more, fine Liaver (0.5–1 mm and 1–2 mm) has a higher crushing strength than coarser Liaver (2.6, and 2.1 MPa, respectively). It is therefore important to select the q value in such a way that a low target density, with the appropriate strength, can be achieved. For lightweight concrete mixes with a density of 850 kg/m^3, a lower distribution factor (q) was used, in order to increase the content of fine Liaver with higher strength and density and to reduce the coarse, low density and low crushing strength. Moreover, the particle density of coarse Liaver aggregate is very low and to achieve the targeted density of 850 kg/m^3, a high amount of high density cement, compared to the lightweight aggregates, must be used. A small distribution factor (q) was therefore selected, so as to increase the content of higher density fine aggregate. Quartz sand was also added to the mixture to achieve the desired density. To improve the strength of the cement paste, as well as the bond between the aggregate and the cement matrix, silica fume and nanosilica was used, as can be seen in Table 5. The maximum lightweight aggregate size was set at 4 mm, since the crushing strength of larger aggregate is significantly lower.

2.3. Mix design

Two groups of LWCs, namely lightweight aggregate concrete (LWAC) with an initial density of 850 kg/m^3 and ultra-lightweight aggregate concrete (ULWAC), with an initial density of 450 kg/m^3, were produced. Cement was replaced with NS in a proportion of 1, 2, 5 and 10 wt-%. Specimens containing nanosilica were designated as NS1, NS2, NS5 and NS10, where the digit describes the amount of NS. Control concretes (C) and concretes containing 10 wt-% of silica fume (SF), as a cement replacement, were prepared for the purposes of comparison. To distinguish between different concrete densities, specimens were additionally labelled with the letters L and U, meaning lightweight or ultra-lightweight, respectively. Accordingly, UNS10 means ultra-lightweight concrete (U) containing 10 wt-% of NS as a cement replacement. The mix proportions have been summarized in Table 1.

2.4. Sample preparation

In the experimental part, 12 mixes were prepared and tested: 6 mixes of both LWAC and ULWAC. Cementitious material content, as well as aggregate grading and content, were constant for each density class. A concrete mixer (Zyklose mixer, Pemat, Germany) with a capacity of 50 L was used to manufacture the concrete. In the mixing process, aggregates, cement and silica fume were mixed in a dry state for 60 s. Water and superplasticizer were then added, after which mixing continued for an additional 60 s. In the case of NS addition, the suspension was mixed together with mixing water and superplasticizer. The viscosity-enhancing admixture was finally added, with everything being mixed for an additional 2 min. Due to problems associated with vibrating fresh lightweight concrete, it was decided not to apply any vibration, and that the concrete produced should be self-leveling. In order to reach this goal the concrete mixture was designed in consistency class of F4/F5 (according to EN 206-1), corresponding to a slump flow diameter of about 500–600 mm. After mixing, concrete consistency was checked by measuring the slump flow diameter, according to EN 12350-5. The flow test was performed without dropping or raising (jolting) as it might affect the stability of the mixture. Moreover, after measuring the flow of the mixture, visual inspection of each mix has been performed in order to satisfy that each concrete mixture does not exhibit potential to bleeding or segregation. After achieving the required consistency class, 150 × 150 × 150 mm^3 and 100 × 100 × 100 mm^3 cubical steel molds, as well as standard 40 × 40 × 160 mm^3 prisms, were filled with fresh concrete without compaction. All the samples were stored in a curing chamber with controlled temperature and relative humidity of 21 ± 1 °C and 99%, respectively, till demolding after 24 h.

2.5. Testing methods

2.5.1. Oven-dry density and thermal conductivity

Oven-dry density and thermal conductivity were determined after curing the samples for 28 d. Oven-dry density was measured following the specifications of EN 12390-7. For this purpose, three 15 × 15 × 15 cm^3 samples of each type of concrete were oven-dried at 105 °C until reaching a constant mass. Afterwards, three mass measurements were performed with the mean value being selected as the dry density.

For thermal conductivity measurements conforming to ISO 22007-2, oven-dried specimens were tested with the transient plane source method (TPS), using a Hot Disk measuring device (Göteborg, Sweden). The TPS method allows rapid, accurate and non-destructive testing of the thermal parameters of various materials, including cement-based composites. Thermal conductivity was measured using a Kapton-insulated sensor placed between two identical 10 × 10 × 10 cm^3 concrete specimens. Each mix design was tested on three groups of specimens, with the mean value taken into consideration in each case.

Table 5
Concrete mixture compositions.

Sample designation	Targeted density [kg/m^3]	Mix proportions [kg/m^3]									
		Cement	Silica fume	Nanosilica suspension	Quartz sand 0.1–0.3 mm	Liaver® 0.5–1 mm	Liaver® 1–2 mm	Liaver® 2–4 mm	Water	SP*	ST**
LC	850	480	–	–	34	79.3	54.4	56.4	192	7.2	0.6
LSF		432	48	–	34	79.3	54.4	56.4	192	8.4	0.6
LNS1		474	–	12	34	79.3	54.4	56.4	186	7.5	0.6
LNS2		468	–	24	34	79.3	54.4	56.4	180	9	0.3
LNS5		456	–	48	34	79.3	54.4	56.4	168	9.5	–
LNS10		432	–	96	34	79.3	54.4	56.4	144	10.8	–
UC	450	200	–	–	–	51.4	60.6	98	140	5.0	0.7
USF		180	20	–	–	51.4	60.6	98	140	6.0	0.7
UNS1		197.5	–	5	–	51.4	60.6	98	138	6.0	0.6
UNS2		195	–	10	–	51.4	60.6	98	135	6.5	0.5
UNS5		190	–	20	–	51.4	60.6	98	130	7.2	0.5
UNS10		180	–	40	–	51.4	60.6	98	120	7.5	0.5

*SP: superplasticizer, **ST: stabilizer.

2.5.1.1. Water accessible porosity and water sorptivity. Water accessible porosity was measured using the water displacement method. Firstly, three 10 × 10 × 10 cm^3 saturated concrete samples were surface dried, with their mass then determined. Next, the samples were dried at 105 °C till reaching a constant mass, after which their dry mass was measured. Porosity was calculated from the difference between the dry and saturated masses, with the value expressed as a percentage.

For calculation of the water absorption coefficient, the water sorptivity test was performed on 40 × 40 × 160 mm^3 sized specimens. The test was performed using the partial immersion method described in EN ISO 15148. Before the test, the specimens were kept in ambient conditions to stabilize their mass, with the sides sealed with hot paraffin wax. Afterwards, specimens were placed in a tank with a constant water level to allow a one directional water uptake process. Three prisms of each type of concrete were dedicated to this part of the experiment, with the weight of specimens determined at specified times up to 24 h. Afterwards, the water absorption coefficient, which describes the ratio between the water quantity absorbed by the specimens per unit area and the square root of time, was calculated.

2.5.1.2. Drying shrinkage. Drying shrinkage represents volumetric changes due to the loss of water from concrete. In this investigation, a standard Graf-Kaufmann method, following DIN 52450, was used to determine the shrinkage behavior of lightweight concrete. Measurement started after demolding at 1 d and continued till 28 d, to get an initial indication about volumetric changes in lightweight concrete. 40 × 40 × 160 mm^3 concrete prisms were used to determine changes in sample lengths. After casting, the samples were stored in a controlled curing chamber with a relative humidity and temperature of 65% and 21 °C, respectively. Shrinkage was measured at 1, 3, 7 and 28 days.

2.5.1.3. RapidAir measurement – 2D imagining technique. A standardized, 2D image-based technique on 15 × 15 cm^3 cubic specimens, using a RapidAir 457 Automated-Air-Void-Analyzer (Concrete Experts International, Sweden) and following EN 480-11:2005, was performed to evaluate the air void characteristics of the hardened concretes. The samples were cut vertically from the middle of the cube, using a water-cooled diamond blade saw, to produce 15 × 15 × 1 cm^3 slices. The samples were then thoroughly polished with polishing powders of different finenesses and then dried. The polished samples were coated with a broad-tipped black marker. After the ink had completely dried, the samples were placed into a 55 °C oven and then removed and coated with white zinc paste (white pigment). After cooling, the excessive paste was removed from the aggregate and cement mortar areas by dragging an angled razor blade across the surface. This produced a polished concrete cross-section which was stained with black ink and in which the voids were filled with a zinc paste, allowing the Rapid Air device to distinguish between air voids and the concrete matrix. The RapidAir device automatically scanned the sample surfaces and provided the air void parameters. Two specimens were tested for each type of concrete, with each sample tested twice. The surface in question had an area of 120 × 80 mm^2, with the traverse from where the reading was taken having a length of 2413.5 mm.

2.5.1.4. X-ray micro-computed tomography (micro-CT). A non-destructive approach – X-ray micro-computed tomography (micro-CT) – was utilized to obtain a detailed investigation of microstructural characteristics. Micro-CT is a non-invasive method that can enable visualization and examination of the internal microstructure of a target material, without damaging it [41,42]. The data obtained from micro-CT can be utilized for investigating pore and solid characteristics.

Fig. 1 presents the micro-CT imaging procedure used for classifying a specific target component from the original micro-CT image. As shown in the 1st image of Fig. 1, a set of resulting images of the specimens are generated using micro-CT; this two-dimensional (2D) image is composed of 500 × 500 pixels with a 29.8 μm pixel size. As can be seen in the figure, the 8-bit original micro-CT image is expressed in greyscale with a number between 0 and 255 (i.e. a total of 256), which is determined according to the relative material density. For example, the black represents pores, while the light and dark grey represent the cement matrix and aggregate solids, respectively.

For more effective characterization, target components such as aggregates and pores were segmented using the multi-thresholding approach [43,44], as well as a modified watershed [35]. Using these methods, aggregate solids (2nd image) and pores

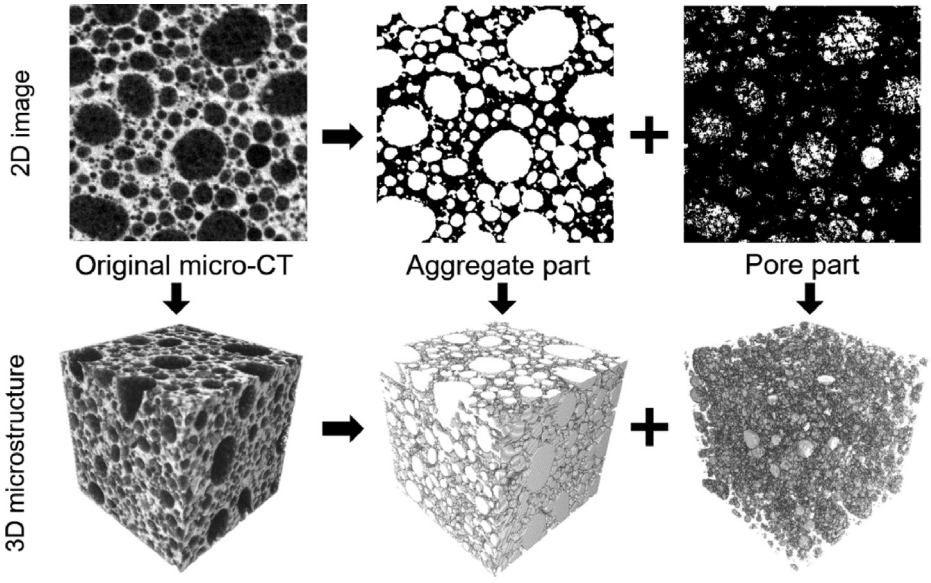

Fig. 1. Micro-CT imaging procedure for classifying target components from the original image, using multi-level thresholds and a modified watershed algorithm (Note: in the images of the aggregate and pore parts, the white represents the target component, while the black is the background.)

(3rd image) were successively classified, making it possible to effectively visualize the 3D microstructures of the aggregates and pores, as shown in Fig. 1. In this study, pore characteristics such as porosity and pore size distribution were examined based on the 3D microstructures obtained from the micro-CT imaging, as shown in the lower part of Fig. 1. In general, the matrix part in the 8-bit micro-CT image is represented in light grey, due to its high solid density. The lightweight aggregates, however, are depicted in dark grey, because of their relatively sparse material density, with the pores represented in black. The use of a multi-threshold method [43,44] and a modified watershed algorithm [35], allowed effective visualization of detailed pore shapes and solid structures. The whole image can be classified into four categories: pores within the matrix and the aggregates, as well as the solid parts of the matrix and the lightweight aggregates. The pores and solid characteristics related to pore structures were of main concern in this study, because these are dominantant in determining material properties.

The wall-thicknesses of the specimens were also computed using their microstructures, so as to evaluate the effects of solid characteristics on material properties. Wall thickness denotes the thickness of the solid structure between pores, particularly between the closest pores. In order to calculate this value, the centroid and radius information of all the pores were examined first. Based on the information obtained, the closest pore from another, selected pore was identified, with the wall thickness between the pores computed by subtracting the radius of each pore from the distance between their centroids. This process was repeated for all the pores, making it possible to obtain the wall thickness distribution.

3. Results and discussion

3.1. Mixture consistency

The consistency of the fresh concrete was determined by measuring the slump flow diameter. As mentioned in Section 2.4., in order to produce a self-leveling, homogeneous mix with a high filling ability, the targeted consistency class was set at F4/F5, which corresponds to a slump flow diameter of about 500–600 mm. Exemplary images of ULWAC and LWAC consistency are presented in Figs. 2 and 3, respectively. The water content of LWAC mixes with a targeted density class of 850 kg/m^3 is higher than what is needed for ULWAC mixes with a lower density class (450 kg/m^3), due to differences in cement content. Superplasticizer was adopted to achieve the required consistency, as can be seen in Table 5. A consistency drop was observed with increasing NS content and consequently higher dosages of superplasticizer were needed. In the preliminary experiments, all the concretes suffered segregation due to density differences between the cement paste and the lightweight aggregate. The addition of stabilizer (viscosity-enhancing admixture) solved the problem of segregation efficiently, with the mixture thus becoming more cohesive and homogeneous. Mixes with NS exhibit better stability than other mixes and therefore lower stabilizer dosages are needed, as mentioned in Table 5. Due to its very fine particle size, NS addition improves the stability and viscosity of a fresh mix. However, consistency is thus negatively affected and consequently higher dosages of superplasticizer were added to achieve the required consistency. It is clear from the dosages added that LWAC needed more superplasticizer than ULWAC, due to the high cement content and the high viscosity of the LWAC mixture. Conversely, ULWAC needed more stabilizer due to the low binder content in the mix resulting in a high possibility of segregation.

3.2. Oven-dry density and thermal conductivity

Fig. 4 presents the experimental results of the oven-dry density tests of different concrete mixes. The targeted densities in both concrete series were achieved to a certain extent. For LWAC, it is clear that all the mixes had a density > 850 kg/m^3, except for mix LNS10. The first three mixes (LC, LNS1, LNS2) had similar dry densities, but when the NS dose was increased to 5 wt-% (LNS5), the density increased significantly > 900 kg/m^3, due to the filling and better packing effects of the very fine NS particles. When the dosage was increased further, to 10 wt-%, the density decreased significantly to 792 kg/m^3. This can be attributed to the high agglomeration potential of NS. Furthermore, mixes with higher NS contents exhibit higher cohesivity and viscosity and consequently the air voids created cannot escape, mainly because compaction is not applied. These factors combined resulted in a significant decrease in the density of mixes with a high NS content. A similar trend was observed for the second group of ultra-lightweight concretes, although this was not the case for concrete containing silica fume (LSF and USF), despite a high SF dosage also being used. This can be attributed to the lower specific surface area of SF, as compared to NS [25], which was also reflected in the amount of plasticizer needed (Table 3).

The experimental thermal conductivity results show that concrete density was mainly correlated to a material property: as can be seen in Fig. 5, it increased with thermal conductivity. ULWAC mixes therefore exhibited substantially lower thermal conductivity when compared to the corresponding LWAC mixes. Compared to dry density, mix composition and fine material prop-

Fig. 2. Images of the ULWAC in the fresh state (mix UC).

Fig. 3. Images of the LWAC in the fresh state (mix LC).

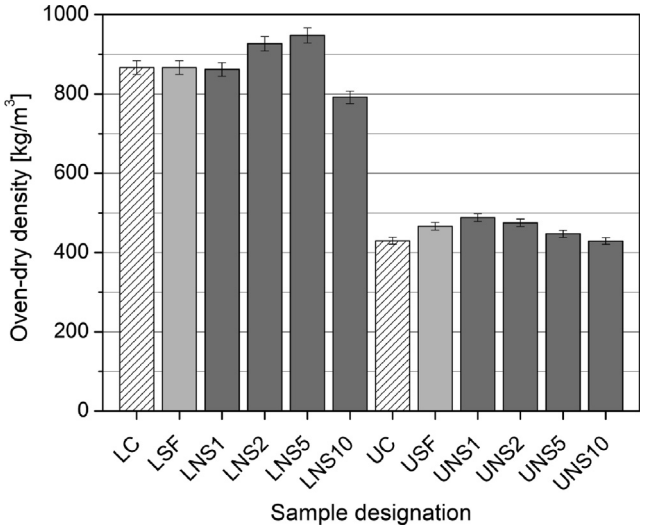

Fig. 4. Experimental results of the dry density tests of the lightweight concrete series.

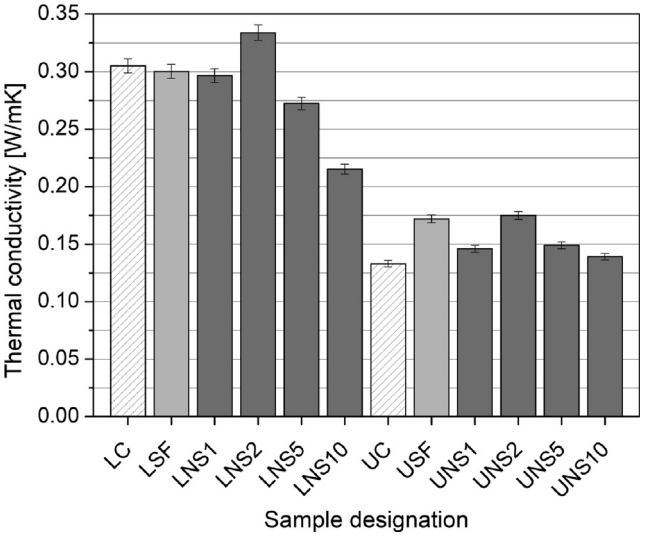

Fig. 5. Experimental results of the lightweight concrete series thermal conductivity tests.

erties have only a marginal influence on thermal conductivity; this being a matter of the ratio between the pore volume and the solid structure volume of concrete. However, pore size distribution and pore shape have only a secondary influence in this regard [43].

3.3. Flexural strength and compressive strength after 28 days of curing

Fig. 6 presents the flexural strengths of two types of concretes after 28 d of curing. It can be seen that ULWAC specimens (Fig. 6a) exhibited lower flexural strengths than the corresponding LWAC (Fig. 6b) mixtures, which is attributable to the increased porosity and lower density of ULWAC. The flexural strength of UC was less than a third of that of LC. It can be seen that the incorporation of silica fume (LSF, USF) in the mixture did not noticeably affect the flexural strength of ULWCs, with values being comparable. However, the incorporation of NS had a beneficial effect in the development of specimens' flexural strengths. Specimen UNS1 exhibited a flexural strength improvement of over 28% when compared to pristine and SF modified specimens (UC and USF, respectively). In the case of LWAC, the effect of NS on flexural strength was more limited, with the flexural strength of LNS2 being only 10% higher than that of LC. Increasing the NS dosage to 5 wt-% led to a gradual strength decrement. However, specimens still exhibited strengths comparable to that of the control specimen. In contrast, specimens with 10 wt-% of NS (UNS10 and LNS10) possessed significantly lower flexural strengths, which is probably correlated with the creation of NS agglomerates and general concrete compaction problems. These results are in line with previous findings: that NS can positively affect the flexural strength of composites by improving the bond between the cement matrix and aggregates to a certain degree, although this effect is not as pronounced as in the case of compressive strength [26,45].

Fig. 7 presents the compressive strengths of concretes after 28 d of curing. Just as in the case of flexural strength, compressive strength decreases significantly with density. The compressive strength value of UC was less than one-fifth of that of the LC specimens. Specimen UC exhibited a compressive strength of almost 3 MPa, while the compressive strength of pristine LC was around 15 MPa. It can be seen that SF-incorporated concretes exhibited a noticeable effect on compressive strength development, which is attributable to SF's filler and pozzolanic activity. The compressive strength of USF increased by 49%, as compared to the control (UC). Strength improvement was also found in the case of LSF, but only by 10%. It can therefore be seen that SF contributed significantly to the strength of both concretes, with the effect being more pronounced in the case of ULWAC. This is most probably attributable to the ability of SF to fill the voids within the cement matrix, which is very loose and porous and more imperfect, as compared to concrete with a higher density. However, it can be seen that the incorporation of NS in much lower dosages than that of SF, led to higher strength improvements. In the case of ULWC (Fig. 7a), while a small amount (1 wt-%) did not contribute to strength improvement, increasing the dosage (up to 5 wt-%) led to noticeable strength increases. Accordingly, the strength of

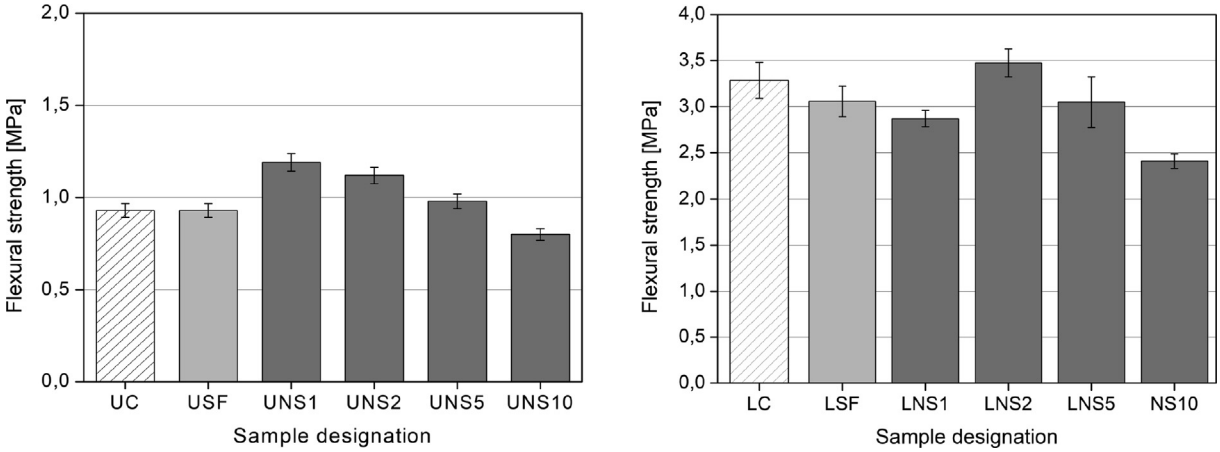

Fig. 6. Flexural strength of ultra-lightweight (left) and lightweight concretes (right) after 28 d of curing.

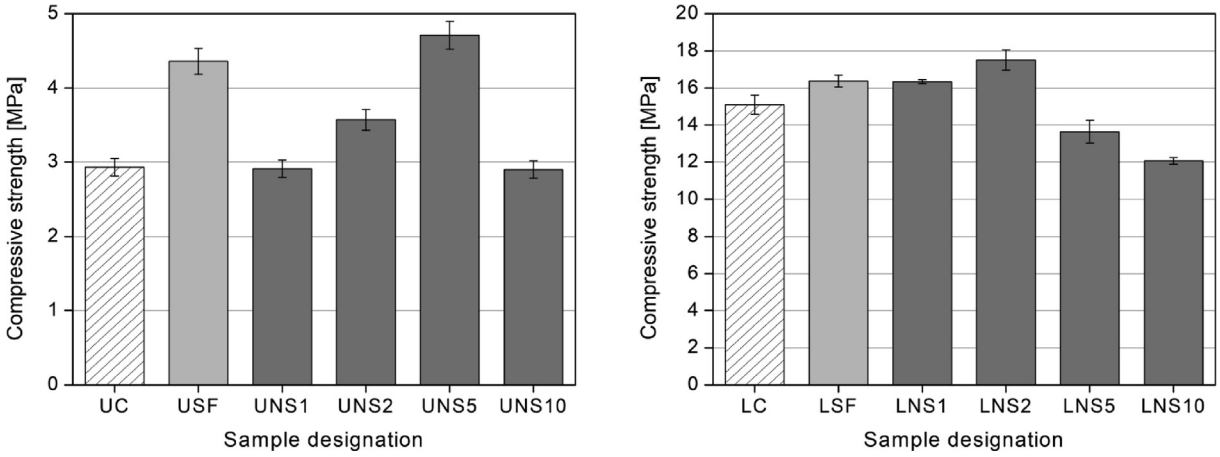

Fig. 7. Compressive strengths of ultra-lightweight (left) and lightweight concretes (right) after 28 d of curing.

UNS5 increased by 61% and 9% compared to UC and USF, respectively. Exceeding the NS dosage (UNS10) resulted in a decrement of strength, leading to the production of concrete with similar strength to that of the control specimen (UC). In the case of LWAC (Fig. 7b), a lower NS dosage was required in order to see beneficial compressive strength effects. The best performance was seen in the case of specimen LNS2, followed by LNS1. In this type of concrete, the strength increased by 17% and 8%, as compared to LC and LSF, respectively. Further addition of NS resulted in a gradual decrement in strength, as a result of inappropriate compaction and problems with workability, which affected the internal composite microstructure of the composite.

These results are in line with the findings of other researchers [13,29–31]; namely, that there is an optimal amount of NS which is beneficial in improving the mechanical properties of cementitious composites. However, the improvement rate depends on the density of the concrete. The present study also confirms the fact that, due to the superior activity of NS as compared SF, a much lower dosage of NS is required to produce a lightweight concrete with comparable or better mechanical performance than one incorporating SF.

3.4. Water accessible porosity and water absorption coefficient

The positive effect of NS on microstructural improvement in lightweight and ultra-lightweight concrete can also be proven by evaluating transport properties, which are often correlated with durability related issues. The results of water porosity, as well as the calculated water absorption coefficient from water sorptivity tests, are presented in Fig. 8. It can be seen that concrete samples with lower densities had significantly increased transport properties as a result of highly increased porosity. The water absorption coefficient and water accessible porosity values of ULWAC (Fig. 8a) were therefore much higher than in the corresponding LWAC (Fig. 8b).

It can be seen that the replacement of cement with 10% of SF significantly improved the microstructure of concretes by decreasing the water accessible porosity. However, in both types of concrete incorporation of NS resulted in the production of a more impermeable microstructure, with NS-modified concretes thus presenting superior transport properties, in comparison to the control and SF-modified specimens. Although exceeding the optimal dosage of NS resulted in a decrement in the beneficial effect of this admixture on water accessible porosity, the water absorption coefficient remained improved. This confirms that NS has a significant role not only in filling the pores of concrete (thus decreasing the total porosity) but that it also refines the pore structure. As reported by other researchers [46–48], the following phenomena occur when NS is present in a cementitious composite: disconnection of continuous pores from discontinuous ones, a subdivision of larger pores into smaller ones and modification of the shape and tortuosity of pores. These result in an improvement in transport

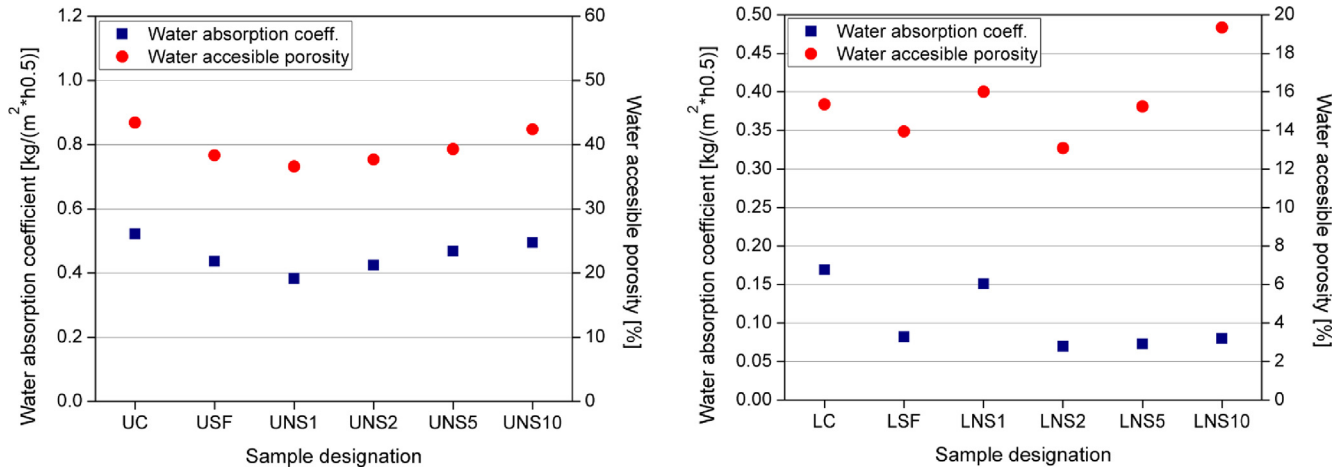

Fig. 8. Water accessible porosity and water absorption coefficient of ultra-lightweight (left) and lightweight concretes (right) after 28 d of curing.

properties, even if NS dosage is excessive, which can lead to a decrement in some properties.

3.5. Drying shrinkage

The investigation focused on drying shrinkage at an early age, due to the high probability of cracking associated with low tensile strength in the first weeks of hydration. The experimental results of drying shrinkage tests are presented in Fig. 9. The presented values are the means of 3 measurements of each mix. All samples were stored in a curing chamber under the same humidity and temperature conditions, since shrinkage measurements are highly affected by these two parameters. It is clear from the results that all the lightweight concrete mixes had drying shrinkages higher than that of traditional concrete [49]. In the two series of lightweight concretes with different densities, several parameters such as aggregate type and content, as well as cement content, influenced the drying shrinkage significantly. ULWAC specimens showed lower shrinkage values than LWAC, which can be attributed to the high paste/aggregate ratio of LWAC, as compared to ULWAC, in spite of the high w/b ratio of the second series (0.7), compared to the first (0.4).

In both series, drying shrinkage increased gradually with time, as can be seen in Fig. 9. However, the addition of fine materials had a significant influence on drying shrinkage. It is clear that drying shrinkage decreased with increases in NS content. NS improves transition zone characteristics and strengthens the bond between the aggregate and cement paste; its addition therefore hinders the movement of water in concrete to a certain extent, thus reducing drying shrinkage [50]. This effect was observed in mixes with the appropriate NS contents, but the influence clearly vanished when the dose was increased to 10 wt-%. This was due to the probability of the agglomeration of very fine particles, which affects the efficiency of nanosilica negatively. Moreover, when compared to SF-modified specimens, concretes with NS exhibited lower shrinkage drying values. The results of our study confirmed the findings of Wang et al. [13], who reported this phenomenon in the case of LWCs, albeit, with much higher concrete densities (Table 1).

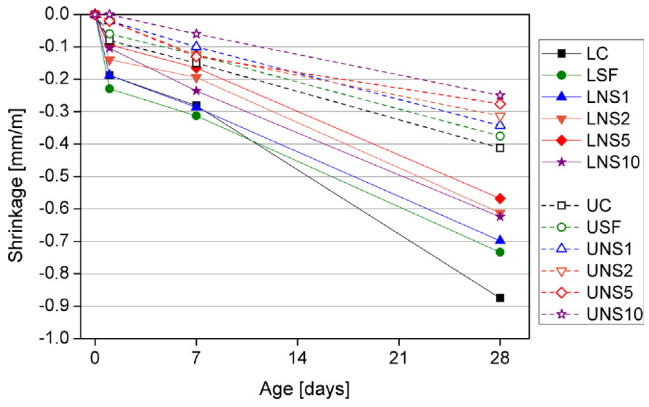

Fig. 9. Experimental results of drying shrinkage tests of lightweight concrete series.

3.6. Microstructural analysis

2D and 3D imagining techniques were utilized to evaluate the effects of NS on the microstructural characteristics of lightweight concrete. Our previous investigations [51,52], as well as the findings of other researchers [53], have confirmed that both investigation techniques show good correlation and accuracy and can thus be applied together to improve evaluation precision and to extend the measurement range. Although the standardized 2D image-based method enables relatively easy measurement, especially when using the automated air void analyser, it requires relatively thin specimens which need to be polished afterwards. As such, porous specimens with low strength cannot withstand the preparation process and therefore only LWAC specimens were measured with the RapidAir device in this study.

As described in Section 3.5.5, both pore and solid characteristics were analysed using the segmented images obtained with micro-CT. Figs. 10 and 11 show the inner pore structures of the specimens used. The general distributions of the pores inside each specimen can be identified in these images. In comparing the LWACs (Fig. 10) and ULWACs (Fig. 11), it can be seen that, in general, more clustered pores exist in the ULWAC specimens; this indicates that lightweight concrete with a lower density tends to have more clustered pores, which affect the mechanical properties of the materials. For a quantitative measurement, porosity values and pore size distributions of the specimens were computed based on the voxel information from the 3D pore images. Since the voxel (pixel) resolution in this study was 29.8 μm, only pores larger than this were taken into consideration.

Fig. 12 shows the porosity measured from the pore structure images in Figs. 10 and 11. Here, each pore was secured by the watershed algorithm and assumed to be a sphere, for more effective pore size measurement. The results in this figure confirm that

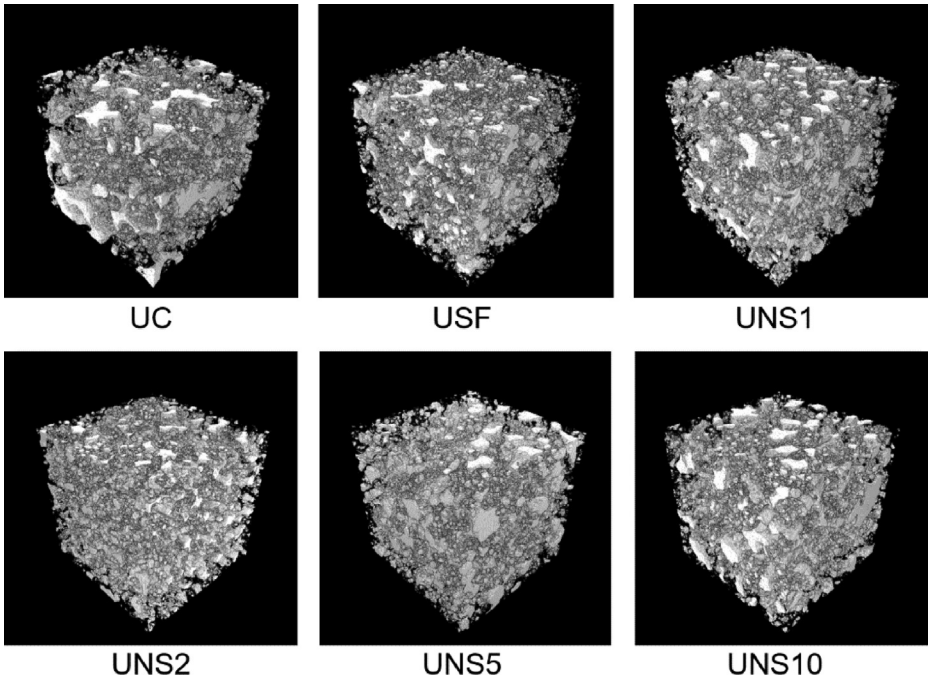

Fig. 10. 3D pore images of ultra-lightweight aggregate concretes (ULWACs).

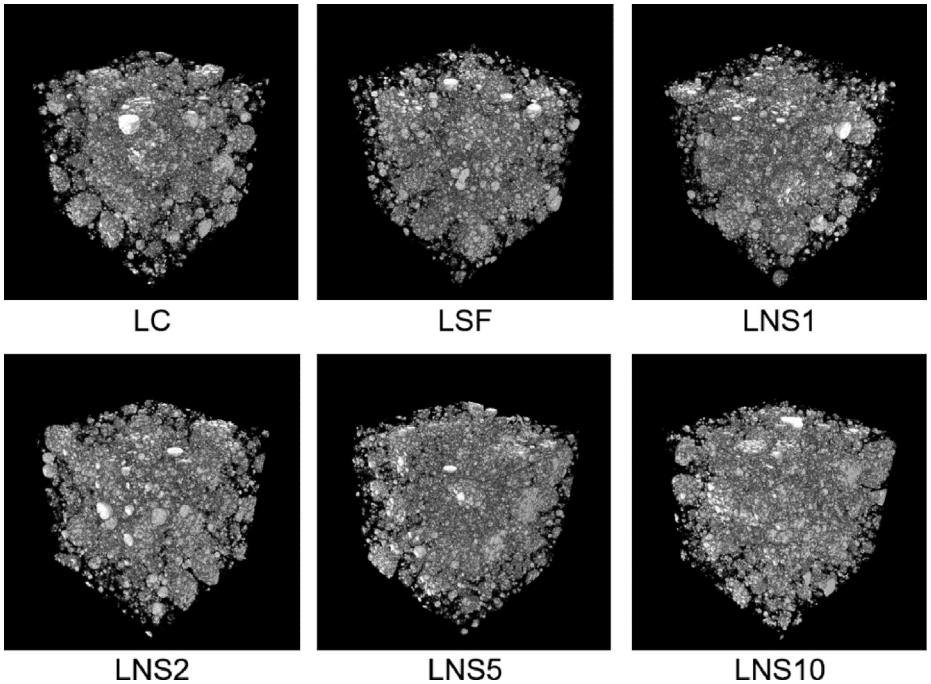

Fig. 11. 3D pore images of lightweight aggregate concretes (LWACs).

ULWAC specimens show larger porosity than LWAC specimens. The porosity of the binder (matrix) was <8% in all cases, with the aggregate porosity being dominant in determining the pore characteristics of the lightweight aggregate concrete. As such, in the case of lightweight aggregate concrete, most of the material characteristics and the properties related to pore structures correlate strongly with the pores in the aggregates. Micro-CT evaluation showed that for both density levels, the specimens with silica fume (LSF and USF) had the lowest porosity in each category within the measured range. Total porosity values obtained for only LWAC with the RapidAir device (Table 6), with a wider measuring range of up to 1 mm, showed a slightly different trend, with the lowest total porosity obtained by LNS2, followed by LSF and then LNS1. However, although the porosities in the two different measuring ranges were slightly different, the overall differences between porosities obtained with both techniques were rather minor. Although it is widely known that porosity is one of the critical factors affecting compressive strength [49,52,54], a direct relationship between the total porosity of specimens and compressive strength was not established in this study. As such, to get a more detailed

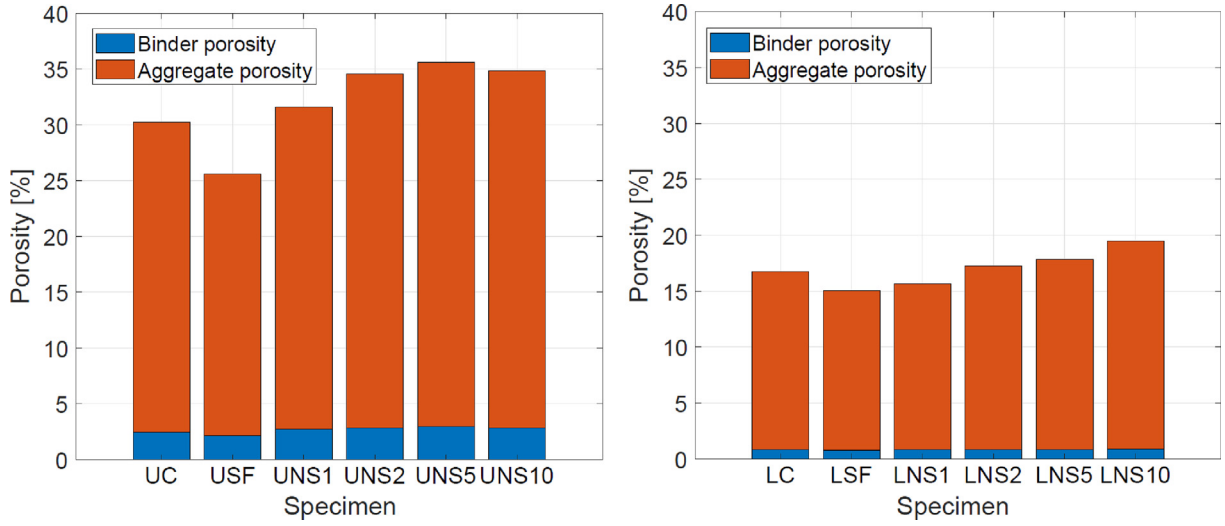

Fig. 12. Measured porosity results of ultra-lightweight (left) and lightweight concretes (right), using micro-CT images.

Table 6
Selected parameters of air-voids measured with RapidAir.

Specimen	LC	LSF	LNS1	LNS2	LNS5	LNS10
Porosity from RapidAir* [%]	32.59	31.16	31.86	29.51	35.33	35.75
Number of voids < 0.5 mm	6027	4906	5075	4518	5443	6727
Number of voids < 1.0 mm	6258	5229	5437	4826	5809	6928
Percent of total number of voids < 0.5 mm	95.7	93.0	92.0	92.4	92.6	96.7
Spacing factor [mm]	0.030	0.034	0.035	0.039	0.030	0.031

*Total porosity up to 1 mm.

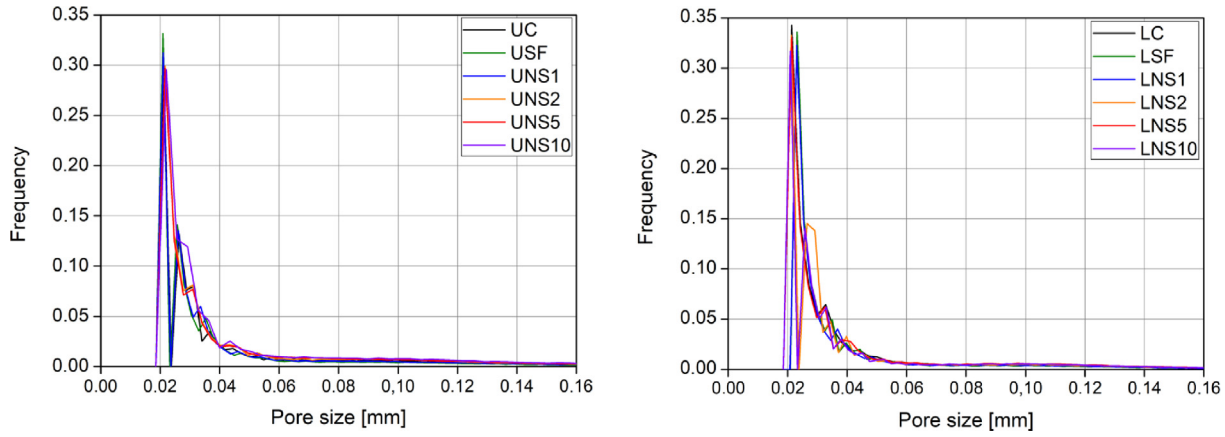

Fig. 13. Pore size distributions of the ultra-lightweight (left) and lightweight concretes (right) obtained with micro-CT.

analysis of pore characteristics, the pore size distributions of the specimens were also investigated, as shown in Fig. 13. However, as the figure shows, there were no clear differences between the pore size distributions of the specimens, regardless of material density or porosity. As a result, another description that can support the pore structures was needed to achieve a better understanding of the material characteristics.

Therefore, in addition to the pore structures, the solid characteristics of the specimens were also examined. Since pore information such as porosity and pore radius can be obtained from segmented CT images, generalized wall thickness, according to the number of voxels, can be computed using pore characteristics. Wall thickness was measured by calculating the distances between the pores' centroids, while taking into account the radius of each associated pore. Fig. 14 shows the wall thickness distribution of the specimens obtained with micro-CT evaluations. In this image, the general distributions of the ULWAC are similar (Fig. 14a). The wall thicknesses of the LWAC specimens (Fig. 14b) are relatively larger than those of the ULWAC specimens, which supports the notion that the strength of the LWAC was higher. In particular, the LNS2 specimen showed a larger wall thickness distribution; this could explain its larger compressive strength, despite the larger porosity. The wall thickness values tended to increase in specimens containing SF and NS, with dosages above 2%; indicating that proper use of NS can contribute to thicker wall thickness, which affects the mechanical properties of cement-based materials.

The micro-CT evaluations can also be confirmed by RapidAir measurements, by analysing the amount of voids counted by the instrument as well as by the spacing factor value. Spacing factor

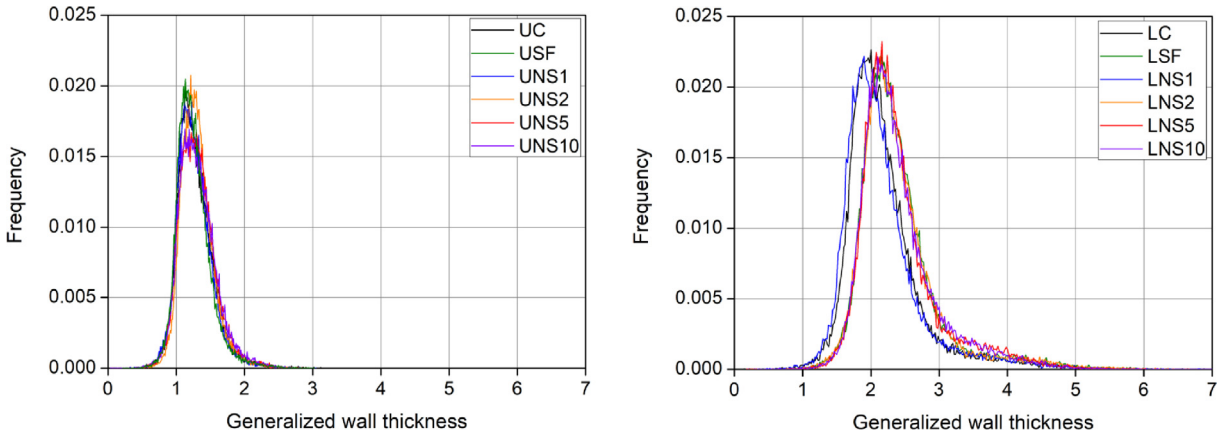

Fig. 14. Wall thickness distributions of the ultra-lightweight (left) and lightweight concretes (right) obtained with micro-CT.

can be simply defined as the distance from the center of a unit cell to the nearest air void surface [55]. RapidAir evaluations (Table 6) revealed that incorporation of both SF and NS in the LWAC mixture, resulted in concrete with less voids, despite total porosities remaining relatively comparable; thus indicating that modification of the specimen skeleton (solid fracture) occurred to a certain extent. The lowest amount of voids counted by the device was in specimen LNS2, followed by LSF and LNS1; this is in line with compressive strength values (Fig. 7). The number of voids increased again with NS dosage, which was reflected in a decrement in the mechanical performance of these specimens. A similar pattern can be observed when analysing the spacing factor value, which confirms that the distance between pores increased with NS dosage up to 2 wt-%. It can thus be assumed that the solid content (thickness of walls) between the pores increased. As discussed earlier, although the total void amount decreased, the total porosity of specimens remained comparable, thus implying that the size of pores should have increased, although this was not proven by micro-CT evaluations (Fig. 13). In analysing the amount of pores counted by RapidAir, it can clearly be seen that the percentage of total number of voids higher than 0.5 mm (above the detection rate of micro-CT) increased noticeably in the specimens, resulting in improved mechanical performance. This could explain why, in the case of ULWAC, no particular trends were observed despite improvements in compressive strength. In addition, due to the very high porosity of ULWAC; differences in specimens' pore characteristics (including alterations in wall thickness) are either very subtle or cannot be tracked, due to the limited resolution of the micro-CT device.

The investigations proved that, in comparison to SF, the incorporation of NS in smaller dosages produces lightweight concretes with a much more robust microstructure and improved mechanical and transport properties. In addition, the study has shown that both imaging techniques can be successfully applied to evaluate the pore characteristics of lightweight concretes and that they show strong a correlation with other results, thus providing good insight into the material characteristics of both ULWAC and LWAC.

4. Conclusions

The following conclusions can be drawn from this work:

- The incorporation of nanosilica (NS) in lightweight aggregate concretes has a significant effect on their fresh properties. Due to the much higher specific surface area of NS, as compared to SF, NS-modified concrete requires a higher dosage of superplasticizer to meet consistency requirements. At the same time, due to the significant increment of viscosity associated with the addition of NS to the mix, a lower amount of stabilizer (or even none) is required to prevent the mixture from bleeding and segregation.
- A noticeable improvement in flexural and compressive strengths after 28 d of curing were reported in both types of concretes, when cement was replaced by NS. Moreover, these specimens exhibited better mechanical performance than SF-incorporated concretes. However, the NS dosage should be carefully adapted, in order to improve the selected properties of the LWAC and ULWAC.
- LWAC concretes exhibited higher shrinkage than ULWACs. Depending on the dosage, nanosilica was found to have a negligible or positive effect on decreasing the drying shrinkage of concretes with its effect more beneficial than the addition of SF to the mixture.
- Both SF and NS have a significant effect on improving the transport properties of concretes by refining the pore structure in the capillary range, thus producing a more impermeable cement matrix. Even when the ideal NS dosage is exceeded, selected transport properties are still improved due to microstructural alteration.
- 2D and 3D imagining techniques confirm that improvements in mechanical performance are attributable to the improvement of void structures in concrete, as a result of increasing concrete wall thickness. Both SF and NS have a substantial effect in the production of a more robust void structure in lightweight concrete. However, the effect of NS is more pronounced even when a lower dosage of the admixture is used.
- The study shows that both 2D and 3D imagining techniques, when applied together, can provide significant insight into the microstructure of lightweight concretes, making it possible to understand the phenomena underlying the mechanisms responsible for improving the mechanical and transport properties of LWCs.

Funding

This project received funding from the European Union's Horizon 2020 research and innovation program, under the Marie Skłodowska-Curie grant agreement No. 841592.

Declaration of Competing Interest

The authors declare that they have no known competing financial interests or personal relationships that could have appeared to influence the work reported in this paper.

Acknowledgement

P. S. is Supported by the Polish Foundation for Science. The authors would like to thank the German Academy of Exchange Services (DAAD), as well as the Egyptian Science and Technology Development Fund (STDF) through the GE-Seed funding program. This work was supported by the Korea Agency for Infrastructure Technology Advancement (KAIA) grant, funded by the Ministry of Land, Infrastructure and Transport (Grant 20NANO-B156177-01). In addition, the authors would like to thank Paul H. Kamm (Helmholtz Centre Berlin) for his assistance in X-ray CT imaging.

References

[1] EN 206-1, Concrete - Part 1: Specification, performance, production and conformity, Aug. 2000.
[2] M. Aslam, P. Shafigh, M.Z. Jumaat, Drying shrinkage behaviour of structural lightweight aggregate concrete containing blended oil palm bio-products, J. Cleaner Prod. 127 (2016) 183–194, https://doi.org/10.1016/j.jclepro.2016.03.165.
[3] S. Choi, Internal relative humidity and drying shrinkage of hardening concrete containing lightweight and normal-weight coarse aggregates: a comparative experimental study and modeling, Constr. Build. Mater. 148 (2017) 288–296, https://doi.org/10.1016/j.conbuildmat.2017.05.057.
[4] M. Gesoğlu, T. Özturan, E. Güneyisi, Shrinkage cracking of lightweight concrete made with cold-bonded fly ash aggregates, Cem. Concr. Res. 34 (7) (2004) 1121–1130, https://doi.org/10.1016/j.cemconres.2003.11.024.
[5] K.-H. Lee, K.-H. Yang, H.-S. Yoon, Shrinkage strains of lightweight aggregate concrete using expanded bottom ash and dredged soil granules, Constr. Build. Mater. 188 (2018) 934–945, https://doi.org/10.1016/j.conbuildmat.2018.08.168.
[6] J.A. Bogas, R. Nogueira, N.G. Almeida, Influence of mineral additions and different compositional parameters on the shrinkage of structural expanded clay lightweight concrete, Mater. Des. 1980–2015 (56) (2014) 1039–1048, https://doi.org/10.1016/j.matdes.2013.12.013.
[7] O. Kayali, M.N. Haque, B. Zhu, Drying shrinkage of fibre-reinforced lightweight aggregate concrete containing fly ash, Cem. Concr. Res. 29 (1999) 1835–1840, https://doi.org/10.1016/S0008-8846(99)00179-9.
[8] J. Silvestre, N. Silvestre, J. de Brito, Review on concrete nanotechnology, Eur. J. Environ. Civ. Eng. 20 (4) (2016) 455–485, https://doi.org/10.1080/19648189.2015.1042070.
[9] L.A. Ivanov, K.E. Razumeev, E.S. Bokova, S.R. Muminova, The inventions in nanotechnologies as practical solutions, Part V. Nanobuild 11 (6) (2020) 719–729, https://doi.org/10.15828/2075-8545-2019-11-6-719-729.
[10] P. Sikora, M. Abd Elrahman, D. Stephan, The influence of nanomaterials on the thermal resistance of cement-based composites-A review, Nanomaterials (Basel) 8 (7) (2018), https://doi.org/10.3390/nano8070465.
[11] L. Varghese, V.V.L.K. Rao, L. Parameswaran, Nanosilica-added concrete: strength and its correlation with time-dependent properties, Proc. Inst. Civ. Eng. Construct. Mater. 172 (2) (2019) 85–94, https://doi.org/10.1680/jcoma.17.00031.
[12] V. Lincy, V.V.L.K. Rao, P. Lakshmy, A study on nanosilica- and microsilica-added concretes under different transport mechanisms, Mag. Concr. Res. 70 (23) (2018) 1205–1216, https://doi.org/10.1680/jmacr.16.00504.
[13] X.F. Wang, Y.J. Huang, G.Y. Wu, C. Fang, D.W. Li, N.X. Han, et al., Effect of nano-SiO2 on strength, shrinkage and cracking sensitivity of lightweight aggregate concrete, Constr. Build. Mater. 175 (2018) 115–125, https://doi.org/10.1016/j.conbuildmat.2018.04.113.
[14] G. Kotsay, Peculiarities of hydration of Portland cement with synthetic nano-silica, Select. Sci. Pap. J. Civ. Eng. 12 (2) (2017) 101–106, https://doi.org/10.1515/sspjce-2017-0025.
[15] M. Samy El-Feky, P. Youssef, A. Maher El-Tair, S. Ibrahim, M. Serag, Effect of nano silica addition on enhancing the performance of cement composites reinforced with nano cellulose fibers, AIMS Mater. Sci. 6 (6) (2019) 864–883, https://doi.org/10.3934/matersci.2019.6.864.
[16] P. Sikora, D. Lootens, M. Liard, D. Stephan, The effects of seawater and nanosilica on the performance of blended cements and composites, Appl. Nanosci. (2020), https://doi.org/10.1007/s13204-020-01328-8.
[17] C. Liu, X. Huang, Y.-Y. Wu, X. Deng, J. Liu, Z. Zheng, et al., Review on the research progress of cement-based and geopolymer materials modified by graphene and graphene oxide, Nanotechnol. Rev. 9 (1) (2020) 155–169, https://doi.org/10.1515/ntrev-2020-0014.
[18] P. Aggarwal, R.P. Singh, Y. Aggarwal, Use of nano-silica in cement based materials—A review, Cogent Eng. 2 (1) (2015), https://doi.org/10.1080/23311916.2015.1078018.
[19] G. Land, D. Stephan, The influence of nano-silica on the hydration of ordinary Portland cement, J. Mater. Sci. 47 (2) (2012) 1011–1017, https://doi.org/10.1007/s10853-011-5881-1.
[20] Krivenko PV, Sanytsky M, Kropyvnytska T. The Effect of Nanosilica on the Early Strength of Alkali-Activated Portland Composite Cements. SSP 2019;296:21–6. https://doi.org/10.4028/www.scientific.net/SSP.296.21.
[21] T. Kropyvnytska, M. Sanytsky, T. Rucinska, O. Rykhlitska, Development of nanomodified rapid hardening clinker-efficient concretes based on composite portland cements, Eastern-Eur. J. Enterprise Technol. 102 (6/6) (2019) 39–48, https://doi.org/10.15587/1729-4061.2019.185111.
[22] K. Skoczylas, T. Rucińska, The effects of low curing temperature on the properties of cement mortars containing nanosilica, Nanobuild 11 (5) (2019) 536–544, https://doi.org/10.15828/2075-8545-2019-11-5-536-544.
[23] S.PH. Jonbi, A. Andreas, A. Nugraha, The long-term effects of nano-silica on concrete, IOP Conf. Ser. Mater. Sci. Eng. 508 (2019) 12038, https://doi.org/10.1088/1757-899X/508/1/012038.
[24] M. Bolhassani, M. Samani, Effect of type, size, and dosage of nanosilica and microsilica on properties of cement paste and mortar, ACI Mater. J. 112 (2) (2015).
[25] H. Biricik, N. Sarier, Comparative study of the characteristics of nano silica - silica fume - and fly ash - incorporated cement mortars, Mat. Res. 17 (3) (2014) 570–582, https://doi.org/10.1590/S1516-14392014005000054.
[26] P. Zhang N. Xie X. Cheng L. Feng P. Hou Y. Wu Low dosage nano-silica modification on lightweight aggregate concrete Nanomaterials and Nanotechnology 8 2018 184798041876128 10.1177/1847980418761283
[27] H. Du, S. Du, X. Liu, Effect of nano-silica on the mechanical and transport properties of lightweight concrete, Constr. Build. Mater. 82 (2015) 114–122, https://doi.org/10.1016/j.conbuildmat.2015.02.026.
[28] N. Atmaca, M.L. Abbas, A. Atmaca, Effects of nano-silica on the gas permeability, durability and mechanical properties of high-strength lightweight concrete, Constr. Build. Mater. 147 (2017) 17–26, https://doi.org/10.1016/j.conbuildmat.2017.04.156.
[29] O. Afzali Naniz, M. Mazloom, Effects of colloidal nano-silica on fresh and hardened properties of self-compacting lightweight concrete, J. Build. Eng. 20 (2018) 400–410, https://doi.org/10.1016/j.jobe.2018.08.014.
[30] M. Abd Elrahman, S.-Y. Chung, P. Sikora, T. Rucinska, D. Stephan, Influence of nanosilica on mechanical properties, sorptivity, and microstructure of lightweight concrete, Materials (Basel) 12 (19) (2019), https://doi.org/10.3390/ma12193078.
[31] H. Du, Properties of ultra-lightweight cement composites with nano-silica, Constr. Build. Mater. 199 (2019) 696–704, https://doi.org/10.1016/j.conbuildmat.2018.11.225.
[32] Q.L. Yu, P. Spiesz, H.J.H. Brouwers, Ultra-lightweight concrete: Conceptual design and performance evaluation, Cem. Concr. Compos. 61 (2015) 18–28, https://doi.org/10.1016/j.cemconcomp.2015.04.012.
[33] P. Vargas, N.A. Marín, J.I. Tobón, Performance and microstructural analysis of lightweight concrete blended with nanosilica under sulfate attack, Adv. Civil Eng. 2018 (2018) 1–11, https://doi.org/10.1155/2018/2715474.
[34] EN 197-1, Cement. Composition, specifications and conformity criteria for common cements, Oct. 2015.
[35] S.-Y. Chung, M. Abd Elrahman, D. Stephan, Effect of different gradings of lightweight aggregates on the properties of concrete, Appl. Sci. 7 (6) (2017) 585, https://doi.org/10.3390/app7060585.
[36] EN 13263-1, Silica fume for concrete. Definitions, requirements and conformity criteria, Sep. 2005.
[37] P. Sikora, K. Cendrowski, M. Abd Elrahman, S.-Y. Chung, E. Mijowska, D. Stephan, The effects of seawater on the hydration, microstructure and strength development of Portland cement pastes incorporating colloidal silica, Appl. Nanosci. (2019), https://doi.org/10.1007/s13204-019-00993-8.
[38] M. Abd Elrahman, B. Hillemeier, Combined effect of fine fly ash and packing density on the properties of high performance concrete: an experimental approach, Constr. Build. Mater. 58 (2014) 225–233, https://doi.org/10.1016/j.conbuildmat.2014.02.024.
[39] R. Yu, D.V. van Onna, P. Spiesz, Q.L. Yu, H.J.H. Brouwers, Development of ultra-lightweight fibre reinforced concrete applying expanded waste glass, J. Cleaner Prod. 20 (2016) 690–701, https://doi.org/10.1016/j.jclepro.2015.07.082.
[40] P.K. Mehta, P.J.M. Monteiro, Concrete: Microstructure, Properties and Materials, 3rd ed., McGraw-Hill, New York, 2005.
[41] N. Bossa, P. Chaurand, J. Vicente, D. Borschneck, C. Levard, O. Aguerre-Chariol, et al., Micro- and nano-X-ray computed-tomography: a step forward in the characterization of the pore network of a leached cement paste, Cem. Concr. Res. 67 (2015) 138–147, https://doi.org/10.1016/j.cemconres. 2014.08.007.
[42] S.-Y. Chung, J.-S. Kim, D. Stephan, T.-S. Han, Overview of the use of micro-computed tomography (micro-CT) to investigate the relation between the material characteristics and properties of cement-based materials, Constr. Build. Mater. 229 (2019), https://doi.org/10.1016/j.conbuildmat.2019.116843 116843.
[43] S.-Y. Chung, M. Abd Elrahman, J.-S. Kim, T.-S. Han, D. Stephan, P. Sikora, Comparison of lightweight aggregate and foamed concrete with the same density level using image-based characterizations, Constr. Build. Mater. 211 (2019) 988–999, https://doi.org/10.1016/j.conbuildmat.2019.03.270.
[44] Z. Yang, W. Ren, R. Sharma, S. McDonald, M. Mostafavi, Y. Vertyagina, et al., In-situ X-ray computed tomography characterisation of 3D fracture evolution and image-based numerical homogenisation of concrete, Cem. Concr. Compos. 75 (2017) 74–83, https://doi.org/10.1016/j.cemconcomp.2016.10.001.
[45] J.-W. Han, J.-H. Jeon, C.-G. Park, Bond characteristics of macro polypropylene fiber in cementitious composites containing nanosilica and styrene butadiene latex polymer, Int. J. Polym. Sci. 2015 (2015) 1–9, https://doi.org/10.1155/2015/207456.
[46] J.I. Tobón, O. Mendoza Reales, O.J. Restrepo, M.V. Borrachero, J. Payá, Effect of pyrogenic silica and nanosilica on portland cement matrices, J. Mater. Civ. Eng. 30 (10) (2018) 4018266, https://doi.org/10.1061/(ASCE)MT.1943-5533.0002482.

[47] G. Quercia, P. Spiesz, G. Hüsken, H.J.H. Brouwers, SCC modification by use of amorphous nano-silica, Cem. Concr. Compos. 45 (2014) 69–81, https://doi.org/10.1016/j.cemconcomp.2013.09.001.
[48] T. Meng, H. Yu, S. Lian, R. Meng, Effect of nano-SiO 2 on properties and microstructure of polymer modified cementitious materials at different temperatures, Struct. Concr. (2019), https://doi.org/10.1002/suco.201900170.
[49] A.M. Neville Properties of concrete 5th ed. 2012 Prentice Hall
[50] H. Du, S.D. Pang, High performance cement composites with colloidal nano-silica, Constr. Build. Mater. 224 (2019) 317–325, https://doi.org/10.1016/j.conbuildmat.2019.07.045.
[51] S.-Y. Chung, M. Abd Elrahman, P. Sikora, T. Rucinska, E. Horszczaruk, D. Stephan, Evaluation of the effects of crushed and expanded waste glass aggregates on the material properties of lightweight concrete using image-based approaches, Materials (Basel) 10 (12) (2017), https://doi.org/10.3390/ma10121354.
[52] S.-Y. Chung, P. Sikora, T. Rucinska, D. Stephan, E.M. Abd, Comparison of the pore size distributions of concretes with different air-entraining admixture dosages using 2D and 3D imaging approaches, Mater. Charact. 162 (2020), https://doi.org/10.1016/j.matchar.2020.110182 110182.
[53] K.Y. Kim, T.S. Yun, J. Choo, D.H. Kang, H.S. Shin, Determination of air-void parameters of hardened cement-based materials using X-ray computed tomography, Constr. Build. Mater. 37 (2012) 93–101, https://doi.org/10.1016/j.conbuildmat.2012.07.012.
[54] H. Garbalińska, J. Strzałkowski, Thermal and strength properties of lightweight concretes with variable porosity structures, J. Mater. Civ. Eng. 30 (12) (2018) 4018326, https://doi.org/10.1061/(ASCE)MT.1943-5533.0002549.
[55] Garboczi EJ, Bentz DP, Snyder KA, Martys NS, Stutzman PE, Ferraris CF et al. An electronic monograph: Modeling and measuring the structure and properties of cement-based materials. Materials and Structural Systems Division, National Institute of Standards and Technology 2014.